

## Effects of Strong Coulomb Correlations on the Phonon-Mediated Superconductivity: A Model Inspired by Copper Oxides

Ju H. Kim and Zlatko Tešanović

*Department of Physics and Astronomy, The Johns Hopkins University, Baltimore, Maryland 21218*

(Received 23 April 1993)

We study how strong Coulomb correlations affect the phonon-mediated superconductivity. Using the Hubbard model representation of a strongly correlated system, we evaluate the Eliashberg electron-pair correlation function for different values of hole doping concentration,  $x$ . The pair interaction is repulsive near half filling ( $x=0$ ), but it becomes attractive above some critical value of  $x$ , making the phonon-mediated superconductivity possible. We also compute the isotope effect coefficient.

PACS numbers: 71.30.+h, 71.27.+a, 74.72.-h

Since the discovery of the high- $T_c$  superconductors, significant progress has been made toward understanding the role of phonons in the normal and superconducting (SC) states of these materials [1]. It is widely believed that the electronic mechanism is dominant in high- $T_c$  systems, but the phonon mechanism is expected to play some role [2] in enhancing the SC transition temperature  $T_c$ . This view is supported by the tunneling and isotope effect data in  $\text{Ba}_{1-x}\text{K}_x\text{BiO}_3$  [3] and an intimate relationship between phonons and  $T_c$  in the cuprates [4]. Furthermore, the recent tunneling and isotope effect,  $\beta_{\text{iso}}$ , data measured in the copper oxides may also support this view. For example, the tunneling measurements in the  $\text{Nd}_{2-x}\text{Ce}_x\text{CuO}_4$  sample [5] indicate that there is a correlation between the peaks in the data and the phonon density of states  $F(\omega)$  at low energies. The isotope effect [6] for the maximum- $T_c$  sample is less than 0.05, but  $\beta_{\text{iso}}$  in reduced- $T_c$  samples from both  $\text{La}_{2-x}\text{Sr}_x\text{CuO}_4$  and Y-Ba-Cu-O (YBCO) systems is not negligible [7]. This evidence led to making the assumption [8] in other studies that electron-phonon interactions are the dominant pairing mechanism within the CuO layer. Hence, it is important to explore the role of phonons in the superconductivity of strongly correlated systems [9]. Examples of such systems are copper oxides, some organic superconductors, and possibly  $\text{C}_{60}$ .

To understand electron-phonon interactions in the cuprates, several attempts [10] have been made to estimate  $\alpha^2F(\omega)$  and  $\beta_{\text{iso}}$ . Those studies, however, are *incomplete* because the strong on-site Coulomb correlations have not been properly included. In characterizing the strength of electron-phonon interactions, strong Coulomb correlation effects are important because they lead to the Mott-Hubbard insulator at half filling and the metallic cuprates evolve from this state [11]. Indeed, strong Coulomb correlations suppress charge fluctuations and thereby reduce the electron-phonon coupling constant as the insulator is approached [12]. To illustrate the correlation effects, we compute the Eliashberg electron-pair correlation function and  $\beta_{\text{iso}}$  as a function of hole doping concentration  $x$ . Our calculation is based on the microscopically derived electron-phonon [ $\alpha^2F(\omega)$ ] and elec-

tron-electron [ $\mu_{SB}^*(\omega)$ ] spectral functions within a particular model of strongly correlated systems.

Our approach is based on the  $1/N$  expansion scheme. The virtues and shortcomings of this approach in studying strongly correlated systems are well known [11,13]. In this Letter, our primary interest is in charge correlations whose qualitative features can be understood within such an expansion scheme. To simplify the calculations but still retain the essential physics, we use the one-band Hubbard Hamiltonian as a model for strongly correlated systems. This model does not place a van Hove singularity in the density of states,  $N(E)$ , at finite values of  $x$  as suggested by more realistic models for copper oxides. The van Hove singularity may enhance [2] the strength of electron-phonon interactions, but we focus only on the Coulomb correlation effects. In the auxiliary boson formulation [13], the Hubbard Hamiltonian is written as

$$H = -t \sum_{\langle ij \rangle, \sigma} (C_{i,\sigma}^\dagger e_i e_j^\dagger C_{j,\sigma} + C_{j,\sigma}^\dagger e_j e_i^\dagger C_{i,\sigma}), \quad (1)$$

where operators  $C_{i,\sigma}^\dagger$  and  $e_i^\dagger$  create the half-full state with spin  $\sigma$  and empty occupation state, respectively. To exclude double occupancy at each sites, we impose the constraint

$$\sum_{\sigma} C_{i,\sigma}^\dagger C_{i,\sigma} + e_i^\dagger e_i = 1 \quad (2)$$

via a Lagrange multiplier  $\lambda_i$ . In the copper-oxygen plane, oxygen orbitals are included via the effective hopping matrix element  $t$  between two sites.

In mean-field theory ( $\langle e_i^\dagger \rangle = \langle e_i \rangle = e_0$  and  $\lambda_i = \lambda_0$ ), Eqs. (1) and (2) lead to a renormalized band structure in which the hybridization  $t$  is substantially reduced, and the bare energy level is raised toward the chemical potential  $\mu$ ,

$$E_{\mathbf{k}} = \lambda_0 - \mu + \frac{r_0^2}{t} \gamma_{\mathbf{k}}. \quad (3)$$

Here,  $\gamma_{\mathbf{k}} = 2(\cos k_x a + \cos k_y a)$ ,  $r_0 = e_0 t / \sqrt{N}$ , and  $N$  is the orbital degeneracy factor. At half filling, the renormalized hybridization vanishes identically, and this signals the breakdown of the Fermi liquid picture.

By introducing a small lattice distortion, we calculate

from Eq. (1) the self-consistent electron-phonon coupling constant that includes the dynamical screening contribution [12,14]. Ionic displacements modulate the hopping matrix element  $t$ . In the harmonic approximation, the modulation of  $t$  is expressed as

$$t(R_{ij}) \approx t(R_{ij}^0) + \frac{\delta t}{\delta R_{ij}} \delta R_{ij}, \quad (4)$$

where  $R_{ij}^0 = R_i^0 - R_j^0$  denotes the distance between ions at equilibrium, and  $\delta R_{ij} = \delta R_i - \delta R_j$  is the relative change in the position of ions at the site  $i$  and  $j$ . The second term in Eq. (4) leads to the electron-phonon interaction Hamiltonian. The  $\mathbf{k}$ -space representation of the electron-phonon Hamiltonian (in mean-field theory) for an arbitrary phonon momentum  $\mathbf{q}$  is expressed as

$$H_{\text{el-ph}} = -\frac{r_0^2}{t^2} \sum_{\mathbf{k}, \mathbf{q}, \sigma, \nu} g_{\mathbf{q}, \nu}^0 \eta_{\mathbf{k}, \mathbf{k}+\mathbf{q}} C_{\mathbf{k}+\mathbf{q}, \sigma}^\dagger C_{\mathbf{k}, \sigma} (a_{\mathbf{q}, \nu}^\dagger + a_{-\mathbf{q}, \nu}), \quad (5)$$

where the  $\mathbf{q}$  dependent parameter is obtained from the second quantization of the displacement vector in Eq. (4),

$$g_{\mathbf{q}, \nu}^0(\mathbf{k}, \mathbf{k}') = g_{\mathbf{q}, \nu}^0 \frac{r_0^2}{t^2} \left[ \eta_{\mathbf{k}, \mathbf{k}'} + \Lambda_r(\mathbf{k}, \mathbf{k}') N \sum_{\mathbf{k}'', \alpha} B_{r\alpha} \Lambda_\alpha(\mathbf{k}'' + \mathbf{q}, \mathbf{k}'') G_{\mathbf{k}''} G_{\mathbf{k}'' + \mathbf{q}} \eta_{\mathbf{k}'', \mathbf{k}'' + \mathbf{q}} \right], \quad (7)$$

where  $B_{\alpha\beta}$  is the slave boson propagator,  $\alpha, \beta = r, \lambda$ , and  $G_{\mathbf{k}} = (i\omega - E_{\mathbf{k}})^{-1}$  is the quasiparticle Green's function.  $\Lambda_r(\mathbf{k}, \mathbf{k}') = -r_0(\gamma_{\mathbf{k}} + \gamma_{\mathbf{k}'})/t$  and  $\Lambda_\lambda(\mathbf{k}, \mathbf{k}') = i$  are the interaction vertex between a quasiparticle and a boson for the  $r$  and  $\lambda$  channels, respectively. It is noted that the second term in Eq. (7) describes the dynamical screening effect.

In order to examine the competition between electron-phonon and effective electron-electron interactions, we calculate the electron-pair interaction function in the Eliashberg scheme [15]. All terms in the perturbation expansion up to  $O(1/N)$  are included. For simplicity, the gap equation is linearized and is expressed in the spectral representation

$$\Delta_{E_{\mathbf{k}}}(i\omega_n) = -\frac{1}{\beta} \sum_{i\omega_m} \int dE_{\mathbf{k}'} I_{E_{\mathbf{k}}, E_{\mathbf{k}'}}(i\omega_m - i\omega_n) C_{E_{\mathbf{k}'}}(i\omega_m) \Delta_{E_{\mathbf{k}'}}(i\omega_m), \quad (8)$$

where  $i\omega_m = i(2m+1)\pi/\beta$  and  $C_{E_{\mathbf{k}}}(i\omega_m - i\omega_n)$  denote the Matsubara frequency for the fermions and Green's function for the pair of electrons, respectively. The contribution from both electron-phonon and electron-electron interactions are included in the pair interaction function

$$I_{E_{\mathbf{k}}, E_{\mathbf{k}'}}(i\omega_m - i\omega_n) = \int_0^\infty d\omega [\alpha^2 F(\omega) - \mu^*(\omega)] \frac{2\omega}{(i\omega_m - i\omega_n)^2 - \omega^2}. \quad (9)$$

Here, the electron-phonon spectral function is given by

$$\alpha^2 F(\omega) = \int_{E_{\mathbf{k}}} (d\mathbf{k}/v_{\mathbf{k}} 4\pi^2) \int_{E_{\mathbf{k}'}} (d\mathbf{k}'/v_{\mathbf{k}'}) \sum_{\nu} |g_{\mathbf{q}, \nu}^0(\mathbf{k}, \mathbf{k}', \omega)|^2 \delta(\omega - \omega_{\mathbf{k}' - \mathbf{k}, \nu}) / \int_{E_{\mathbf{k}}} (d\mathbf{k}/v_{\mathbf{k}}), \quad (10)$$

and the electron-electron (slave boson) spectral function due to the on-site Coulomb repulsion is written as

$$\mu_{SB}^*(\omega) = \int_{E_{\mathbf{k}}} (d\mathbf{k}/v_{\mathbf{k}} 4\pi^2) \int_{E_{\mathbf{k}'}} (d\mathbf{k}'/v_{\mathbf{k}'} \pi) \sum_{\alpha, \beta} \text{Im}[\Lambda_\alpha(\mathbf{k}, \mathbf{k}') B_{\alpha\beta} \Lambda_\beta(\mathbf{k}', \mathbf{k})] / \int_{E_{\mathbf{k}}} (d\mathbf{k}/v_{\mathbf{k}}), \quad (11)$$

where  $v_{\mathbf{k}}$  is the quasiparticle velocity. We evaluate Eqs. (10) and (11), numerically, at the Fermi surface (i.e.,  $E_{\mathbf{k}} = E_{\mathbf{k}'} = E_F$ ). It is noted that the resolution of our calculation is the  $100 \times 100$  mesh points for the Brillouin zone.

The calculated  $\alpha^2 F(\omega)$  for  $x=0.146$  (solid), 0.212 (dotted), and 0.368 (dashed lines) are plotted in Fig. 1(a). Because of difficulties in estimating both  $|g_{\mathbf{q}, \nu}^0|$  and  $F(\omega)$  from the simple model, we choose for definiteness  $|g_{\mathbf{q}, \nu}^0| = 2.3$  and use the measured [16]  $F(\omega)$  for

$$\eta_{\mathbf{k}, \mathbf{k}+\mathbf{q}} = \sum_{b=x, y} \hat{R}_b \hat{e}_{\mathbf{q}, \nu} [\sin k_b a - \sin(k_b + q_b) a]. \quad (6)$$

Here,  $a_{\mathbf{q}, \nu}^\dagger$  ( $a_{\mathbf{q}, \nu}$ ) and  $\hat{e}_{\mathbf{q}, \nu}$  denote the creation (annihilation) operator for a phonon with momentum  $\mathbf{q}$  at branch  $\nu$  and the polarization vector, respectively. The magnitude of  $\eta_{\mathbf{k}, \mathbf{k}'}$  depends strongly on the phonon momentum: It vanishes at  $\mathbf{q}=0$  (uniform displacement) and it reaches its maximum value at  $\mathbf{q}=(1,1,0)\pi/a$  (this corresponds to the Peierls distortion). The bare electron-phonon coupling constant is given by  $|g_{\mathbf{q}, \nu}^0| = 2q_0(2\rho\omega_{\mathbf{q}, \nu})^{-1/2}$ , where  $\rho$  is the mass density and  $q_0 = (1/t)\delta t/\delta R_{ij}$ .  $q_0$  measures the changes in the hopping matrix element  $t$  due to small displacements.

The factor  $r_0^2/t^2$  in Eq. (5) comes from the Coulomb renormalization of the bare coupling  $|g_{\mathbf{q}, \nu}^0|$ . However, the self-consistent electron-phonon coupling constant must include additional electronic screening contributions from the response of the variational parameters  $r_0$  and  $\lambda_0$  to a lattice distortion [12]. This contribution is represented by the diagram with selected channels of the slave boson propagator and the particle-hole bubble [11,12]. The screened electron-phonon coupling is written explicitly as

$\text{La}_{1.85}\text{Sr}_{0.15}\text{CuO}_4$ . (Our choice  $|g_{\mathbf{q}, \nu}^0| = 2.3$  fits the isotope effect data discussed below.) The complex  $x$  dependence in the spectral weight at low frequencies can be understood by decomposing the coupling parameter  $\alpha^2$  into the contributions from (i)  $|g_{\mathbf{q}, \nu}^0|^2$ , (ii)  $N(E_F)$ , and (iii) Fermi surface effects. The contributions from (i) and (ii) are deduced by counting the powers of the Bose amplitude  $r_0$  in Eq. (10). Since  $|g_{\mathbf{q}, \nu}^0|^2 \propto r_0^4$  and  $N(E) \propto r_0^{-2}$ , the combined contributions of (i) and (ii) lead to  $r_0^2 \propto x$ . As  $x$  in-

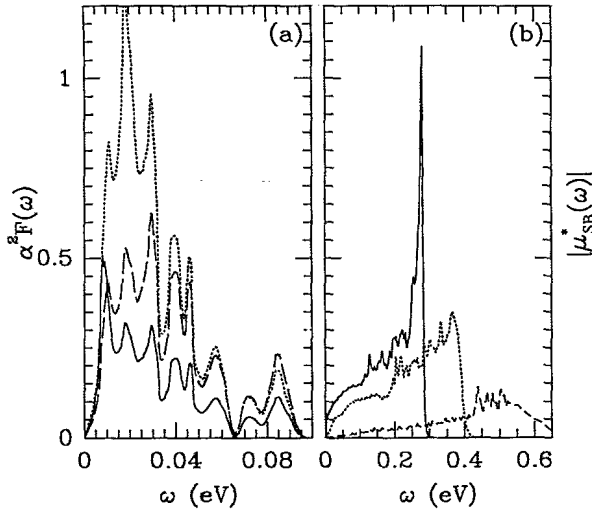


FIG. 1. The calculated (a) electron-phonon and (b) electron-electron spectral functions. The solid, dotted, and dashed lines represent  $x=0.146$ ,  $0.212$ , and  $0.368$ , respectively. The measured phonon density of states  $F(\omega)$  from Ref. [16] is used in the calculation of (a).

creases, the effect from (iii), however, leads to a monotonic decrease in  $\alpha^2$  due to the reduction in the Fermi surface size. For instance, as the Fermi surface shrinks from the square shape of the half-filled band,  $\eta_{\mathbf{k},\mathbf{k}+\mathbf{q}}$  becomes reduced because a smaller  $\mathbf{q}$  vector connects states on the Fermi surface.

The electron-electron spectral functions for  $x=0.146$  (solid),  $0.212$  (dotted), and  $0.368$  (dashed lines) are plotted in Fig. 1(b). The structures in the figure come from the complex frequency dependence of slave boson spectral functions. As  $x$  increases,  $\mu_{SB}^*(\omega)$  is spread over a wider range of frequencies due to the increase in the slave boson dispersion. The distribution of spectral weight follows from the acoustic phononlike behavior of the slave bosons. The  $x$  dependence of  $\mu_{SB}^*(\omega)$  is understood also in terms of (1) the electron-electron interactions,  $\text{Im}[\Lambda_{\alpha} B_{\alpha\beta} \Lambda_{\beta}]$ , (2)  $N(E_F)$ , and (3) the Fermi surface effect. The overall contribution of (1) and (2) estimated by counting powers of  $r_0$  in Eq. (11) shows that  $\mu_{SB}^*(\omega)$  decreases monotonically with  $x$  because the contribution from (1) is roughly concentration independent.

In Fig. 2,  $\lambda_{ph}$  and  $|\mu_{SB}^*|$  are plotted as a function of  $x$ . These parameters are obtained by first setting  $i\omega_n = i\omega_m$  in Eq. (9) and then computing  $\lambda_{ph} = 2 \int d\omega \alpha^2 F(\omega) / \omega$  and  $\mu_{SB}^* = 2 \int d\omega \mu_{SB}^*(\omega) / \omega$ , respectively. In computing  $\lambda_{ph}$ , a low energy cutoff of 11 meV is imposed to consider only the motion from copper and oxygen atoms. The  $x$  dependence of  $\lambda_{ph}$  and  $|\mu_{SB}^*|$  directly reflect the trend in  $\alpha^2 F(\omega)$  and  $\mu_{SB}^*(\omega)$ . The electron-pair interaction function  $I_{pair} = \lambda_{ph} - \mu_{SB}^*$  near the insulator phase is repulsive because of strong effective electron-electron and weak electron-phonon interactions. As  $x$  increases, however, effective Coulomb repulsion becomes weaker while the electron-phonon interaction becomes stronger. At some

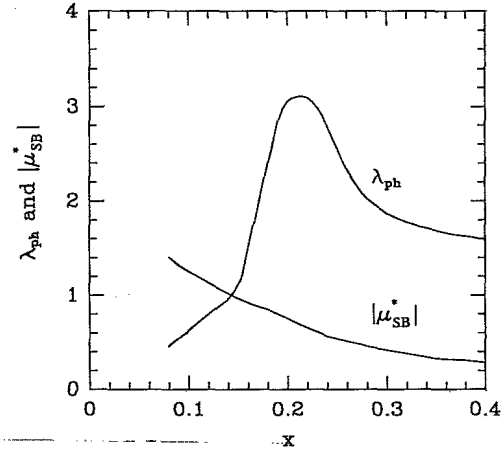


FIG. 2. The  $x$  dependence of the electron-phonon coupling constant  $\lambda_{ph}$  and the effective Coulomb repulsion  $\mu_{SB}^*$ . The bare coupling constant  $|g_{\mathbf{q},\nu}^0|=2.3$  is used in the  $\lambda_{ph}$  calculation.

$x_c$  these two competing interactions cancel each other; hence, for  $x > x_c$ , the pair interaction becomes attractive, and phonon-induced superconductivity becomes possible. The value of  $x_c$ , however, depends strongly on the choice of  $|g_{\mathbf{q},\nu}^0|$ : For example,  $x_c \approx 0.14$  if  $|g_{\mathbf{q},\nu}^0|=2.3$ , and  $x_c \approx 0.24$  if  $|g_{\mathbf{q},\nu}^0|=1.0$ . The former choice leads to  $\lambda_{ph}$  which is consistent with the tunneling data [17], but this is roughly 10 times larger than the value suggested by transport data [18].

Because the small isotope effect is taken as evidence that phonons do not play a role in superconductivity, we estimate the effects of Coulomb correlations on  $\beta_{iso}$  to show the correlation between the strength of the pair interaction and the isotope effect. We follow the formulation [19] of Rainer and Culetto and express  $\beta_{iso}$  in terms of the functional derivative of  $T_c$  with respect to  $\alpha^2 F(\omega)$ . For simplicity, the *square-well* approximation [1] is used (by including only the self-energy contributions from electron-phonon interactions) in the expression

$$\beta_{iso} = \int_0^\infty d\bar{\omega} \frac{\alpha^2 F(\bar{\omega})}{1 + \lambda_{ph}} \sum_n \frac{16\pi^2 n^2 \bar{\omega}}{[4\pi^2 n^2 + \bar{\omega}^2]^2} \Xi_n, \quad (12a)$$

where

$$\Xi_n = \frac{1}{2} \sum_{m,\delta} \pm \left[ \frac{1}{|a_m|} \frac{1}{|a_m + \delta n|} - \frac{\text{sgn}(a_m a_{m+\delta n})}{|a_m + \delta n|^2} \right]. \quad (12b)$$

Here  $a_m = 2m + 1$ ,  $\bar{\omega} = \omega/k_B T_c$ ,

$$T_c = 1.13 \omega_c \exp[-(1 + \lambda_{ph})/(\lambda_{ph} - \mu_{SB}^*)],$$

and  $\omega_c$  is the cutoff frequency for a mediating boson (i.e., phonon). The  $x$  dependence of  $\beta_{iso}$  arises from the particle renormalization factors  $1 + \lambda_{ph}$ ,  $\alpha^2 F(\omega)$ , and  $T_c$ . Because of the complex  $x$  dependence of all three contributions, we evaluate Eqs. (12) numerically by using the spectral functions shown in Fig. 1.

The calculated  $\beta_{iso}$  as a function of  $T_c/T_c^{\text{max}}$  is plotted

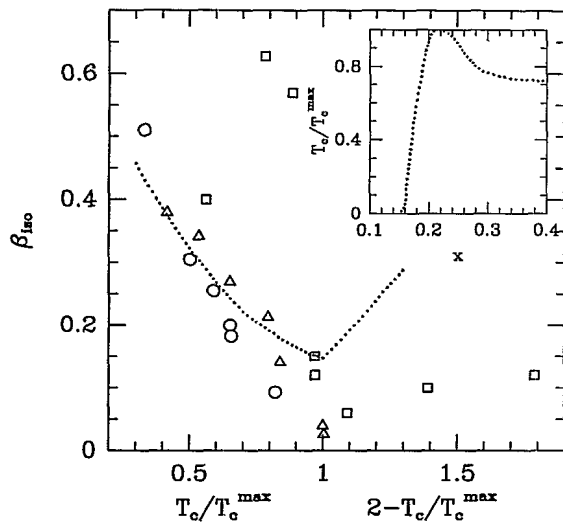


FIG. 3. The isotope effect as a function of  $T_c/T_c^{\max}$ . The dotted line denotes the theoretical result for  $|g_{q,v}^0|=2.3$  and  $\omega_c=96$  meV. Open squares, triangles, and circles denote the data from Refs. [7(a)], [7(b)], and [7(c)], respectively. The normalized  $T_c$  as a function of  $x$  shown in the inset is calculated from the parameters in Fig. 2.

in Fig. 3. The dotted line represents the result for  $|g_{q,v}^0|=2.3$  and  $\omega_c \approx 96$  meV. The plot of  $T_c/T_c^{\max}$  versus  $x$  as shown in the inset illustrates a rapid rise of  $T_c$  to the maximum value and then a gradual decrease as  $x$  increases. This trend is in qualitative agreement with experiments; however, the choice of parameters overestimates the phonon contribution to  $T_c$ . The main figure shows the correlation between  $\beta_{\text{iso}}$  and  $T_c$ :  $\beta_{\text{iso}}$  increases as  $T_c$  decreases, and  $\beta_{\text{iso}}$  has its minimum value at  $T_c=T_c^{\max}$ . This trend is in fair agreement with data [6,7] for  $\text{La}_{2-x}\text{Sr}_x\text{CuO}_4$ ,  $(\text{Y}_{1-x}\text{Pr}_x)\text{Ba}_2\text{Cu}_3\text{O}_{7-\delta}$ , and  $\text{YBa}_{2-x}\text{La}_x\text{Cu}_3\text{O}_7$  samples as represented by open squares, triangles, and circles, respectively. The interpretation of the correlation between  $\beta_{\text{iso}}$  and  $T_c$  based on  $I_{\text{pair}}$  shown in Fig. 2 suggests that  $\beta_{\text{iso}}$  becomes large when the pair interaction is weakly attractive but becomes small when the interaction is strongly attractive.

Our calculation leads to two main results. First, strong Coulomb correlations may not completely suppress the phonon mechanism in the large doping regime. However, the phonon contribution to  $T_c$  calculated in this work may overestimate its actual size in the copper oxides because our procedure gives  $\omega_c=96$  meV. Second, the isotope effect is inversely correlated with  $T_c$ . This suggests that the small  $\beta_{\text{iso}}$  may not necessarily imply the absence of electron-phonon interactions. Consequently, the role of phonons in superconductivity should not be neglected on the basis of strong Coulomb correlations alone. In the case of copper oxides, however, it is important to stress that the contribution of purely electronic mechanisms must be included in any quantitative analysis. Such non-phonon mechanisms [20] may play an important role in the cuprates, particularly in the ones with high transition

temperatures, where strong spin fluctuations may induce unconventional SC states. Similarly, in a heavy fermion superconductor such as  $\text{UPt}_3$ , the nonphononic mechanisms are expected to play a dominant role. In conjunction with this, we expect that, if  $\omega_c > e_0^2 t$ , the phonon-mediated superconductivity will be removed even from a region of moderate doping.

Many useful conversations with K. Levin and Y. Bang are acknowledged. This work was supported by the David and Lucile Packard Foundation.

- 
- [1] J. P. Carbotte, *Rev. Mod. Phys.* **62**, 1027 (1990).
  - [2] D. M. Newns *et al.*, *Phys. Rev. Lett.* **69**, 1264 (1992).
  - [3] J. F. Zasadzinski *et al.*, *Physica (Amsterdam)* **158C**, 519 (1989); C. K. Loong *et al.*, *Phys. Rev. Lett.* **66**, 3217 (1991).
  - [4] S. L. Cooper *et al.*, *Phys. Rev. B* **37**, 5920 (1988); S. Battacharya *et al.*, *Phys. Rev. B* **37**, 5901 (1988); S. J. Hagen *et al.*, *Phys. Rev. B* **40**, 9389 (1989). However, we do not imply here that the superconductivity in copper oxides is phonon mediated. The electron-phonon interaction is only a part (possibly less important) of the complete picture.
  - [5] Q. Huang *et al.*, *Nature (London)* **347**, 369 (1990).
  - [6] L. C. Bourne *et al.*, *Phys. Rev. B* **36**, 3990 (1987).
  - [7] (a) M. K. Crawford *et al.*, *Phys. Rev. B* **41**, 282 (1990); (b) J. P. Franck *et al.*, *Phys. Rev. B* **44**, 5318 (1991); (c) H. J. Bornemann and D. E. Morris, *Phys. Rev. B* **44**, 5322 (1991).
  - [8] S. Chakravarty, A. Sudbø, P. W. Anderson, and S. Strong, *Science* **261**, 337 (1993).
  - [9] The principles governing the interplay between the Coulomb and phonon interactions are discussed in V. L. Ginzburg and D. A. Kirzhnits, *High Temperature Superconductivity* (Plenum, New York, 1982). See also P. Morel and P. W. Anderson, *Phys. Rev.* **125**, 1263 (1962); M. Grabowski and L. J. Sham, *Phys. Rev. B* **29**, 6132 (1984).
  - [10] W. Weber, *Phys. Rev. Lett.* **58**, 1371 (1987); C. C. Tsuei, *Phys. Rev. Lett.* **65**, 2724 (1990).
  - [11] J. H. Kim, K. Levin, and A. Auerbach, *Phys. Rev. B* **39**, 11633 (1989); G. Kotliar, P. A. Lee, and N. Read, *Physica (Amsterdam)* **153-155C**, 538 (1988).
  - [12] J. H. Kim *et al.*, *Phys. Rev. B* **44**, 5148 (1991).
  - [13] P. Coleman, *Phys. Rev. B* **35**, 5072 (1987); N. Read and D. M. Newns, *J. Phys. C* **16**, 3273 (1983).
  - [14] S. Barisic, J. Labbe, and J. Friedel, *Phys. Rev. Lett.* **25**, 919 (1970).
  - [15] G. M. Eliashberg, *Zh. Eksp. Teor. Fiz.* **38**, 966 (1960) [*Sov. Phys. JEPT* **11**, 696 (1960)].
  - [16] B. Renker *et al.*, *Z. Phys. B* **67**, 15 (1987).
  - [17] J. M. Valles, Jr. *et al.*, *Phys. Rev. B* **44**, 11986 (1991).
  - [18] M. Gurvitch and A. T. Fiory, *Phys. Rev. Lett.* **59**, 1337 (1987).
  - [19] D. Rainer and F. J. Culetto, *Phys. Rev. B* **19**, 2540 (1979).
  - [20] For a recent review, see J. R. Schrieffer, *Phys. Scr.* **T42**, 5 (1992).